NASA Technical Memorandum 78733

# Recent Experiences With Three-Dimensional Transonic Potential Flow Calculations

David A. Caughey
*Cornell University, Ithaca, New York*
Perry A. Newman
*Langley Research Center, Hampton, Virginia*
Antony Jameson
*New York University, New York, New York*

National Aeronautics
and Space Administration

**Scientific and Technical
Information Office**

1978

## SUMMARY

Some recent experiences with computer programs capable of solving finite-difference approximations to the full potential equation for the transonic flow past three-dimensional swept wings and simple wing-fuselage combinations are discussed. The programs which have been used are

1. A nonconservative program for swept wings (FLO-22),
2. A quasi-conservative finite-volume program capable of treating swept wings mounted on fuselages of slowly varying circular cross section (FLO-25),
3. A fully conservative finite volume scheme capable of treating swept wings and wing-cylinder combinations (FLO-27).

The present capabilities of these codes are reviewed. The relative merits of the conservative and nonconservative formulations are discussed, and the results of calculations including corrections for the boundary-layer displacement effect are presented. The potential impact of the programs on design will be assessed, considering questions of accuracy, computer cost, and geometric capability, both for the current codes and planned future developments.


## INTRODUCTION

In recent years, finite-difference methods have yielded accurate solutions for the transonic potential flow about a variety of geometries of practical interest to the aircraft designer. The earliest solutions for the full potential problem (as opposed to its transonic small-disturbance approximation) were based upon explicit transformation of the equation to a new system of curvilinear, boundary-conforming coordinates. This technique has been applied successfully to a number of geometries, including airfoils (refs. 1,2), nacelle inlets (ref. 3), and yawed (ref. 4) and swept wings (ref. 5). More recently, the need to describe the mesh-generating transformations analytically and to transform the equation explicitly for each new class of geometries has been circumvented by the introduction of the so-called finite-volume techniques (refs. 6,7) in which the transformation derivatives required at each point are considered purely local functions to be determined numerically from the Cartesian coordinates of the grid points. This decoupling of the solution process from the mesh-generating scheme effectively broadens the geometric applicability of such methods to any configuration for which a convenient boundary-conforming coordinate system can be devised.

The purpose of this paper is to present results of some of these methods which demonstrate the successes of the earlier explicit transformation methods,

and the promise of the newer finite-volume methods for the calculation of the transonic flow past swept-wing and swept-wing/body configurations.

Specifically, the results of three computer codes will be discussed. They are

1. FLO-22, a well-tested operational code capable of solving for the potential flow about yawed or swept wings of arbitrary planform and section shape. The code is based on an explicit transformation of the potential equation into a boundary-conforming coordinate system generated by a sequence of shearing transformations and a simple parabolic conformal mapping. The difference scheme is based on the quasi-linear form of the equation, and is, therefore, nonconservative,

2. FLO-25, a pilot code capable of treating the flow about a wing of arbitrary planform and section shape mounted on a fuselage of circular cross section. The cross-sectional area of the fuselage is allowed to vary in the streamwise direction, but the body must extend to infinity both upstream and downstream as a cylinder of finite (non zero) radius. A finite-volume formulation of the quasi-linear form of the equation is used, but the artificial viscosity (necessary for stability in locally supersonic regions) is added in conservation form. Such a difference scheme can be termed quasi-conservative.

3. FLO-27, a pilot code capable of treating the flow about an arbitrary yawed wing or a swept wing mounted either on a wall (symmetry plane) or on an infinitely long circular cylinder. A finite-volume scheme is used to difference the continuity equation in conservation form.

Use of trade names or names of manufacturers in this report does not constitute an official endorsement of such products or manufacturers, either expressed or implied, by the National Aeronautics and Space Administration.

This work was sponsored in part by NASA and the Office of Naval Research.

## PROGRAM DESCRIPTIONS

A brief description of each of the programs will be given in this section. Since the main purpose of this paper is to describe the general capabilities of the programs and some of the results that have been obtained to date, these descriptions will be necessarily brief. For further details, the reader is referred to References 5, 6, and 7 which describe the numerical analyses upon which the programs FLO-22, FLO-25, and FLO-27, respectively, are based.

Several features of primary importance to the user are summarized in Table I for the three programs. Each of the programs solves a finite-difference approximation to the full potential equation by an iterative relaxation procedure. To speed convergence of this process, the solutions are typically calculated on a succession of grids, each containing twice the number of mesh cells of the preceding grid in each coordinate direction. The computing time

required depends on a number of factors, including the number of mesh points in the supersonic regions of the flow field. The approximate computing times shown in Table I are for a typical case using 100 relaxation sweeps on each of the three grids, with the final grid consisting of 81 920 cells[1]. The programs are designed to store the solution and grid coordinates on an external disk, buffering the values into the central, high-speed core only as they are needed during the solution process. This allows the solution to be calculated on relatively fine grids on a machine with a modest amount of high-speed core.

The three programs are similar in a number of respects. Each uses sequences of simple conformal mappings and shearing transformations to define a boundary-conforming grid system, and solves a finite-difference approximation to the full potential equation. The potential approximation is generally thought not to introduce serious errors as long as shock strengths do not exceed those corresponding to upstream normal Mach numbers of about 1.3. A linearized treatment of the vortex sheet, which ignores its convection and roll-up, is used. The vortex sheet is assumed to lie in a surface near the plane of the wing and to leave the trailing edge smoothly. A constant discontinuity in potential is assumed to exist across the sheet at each spanwise station; the value of the discontinuity is determined by the Kutta condition at the wing trailing edge.

The analysis of FLO-22 is based upon a direct transformation of the usual quasi-linear form of the potential equation to the boundary-conforming coordinate system. This allows most of the transformation derivatives to be calculated analytically and results in a highly efficient computer code. The transformation sequence is based on a simple square-root mapping in each spanwise plane about a point just inside the leading edge of the streamwise section; this reduces the wing surface to a shallow bump which is then sheared out. The details of the wing geometry are contained in this final shearing transformation, which is calculated numerically from the input data. A finite-difference approximation to the transformed potential equation is solved using the "rotated" difference scheme introduced by Jameson (ref. 4). The numerical scheme is very reliable, and the code has been run successfully by many users on a number of different computers for a wide variety of wing geometries. The finite-difference approximation is second-order accurate in subsonic zones but only first-order accurate in supersonic zones. Since the artificial viscosity is added implicitly in the formulation of the rotated scheme, the solutions do not satisfy mass conservation when shock waves are present.

The analysis of FLO-25 is based on a numerical calculation of the required transformation derivatives at each point, although (for convenience) the coordinates of the finite-difference grid are generated in a manner similar to that used in FLO-22. The necessary sequence of transformations is somewhat more complicated to account for an axisymmetric fuselage of varying cross-sectional area and is based on the "wind-tunnel" transformation suggested by Caughey & Jameson (ref. 8). This is applied in concentric cylinders about the fuselage axis after the streamwise variation in cross-sectional area has been sheared out. By the time this level of geometrical complexity is reached, the

[1]The FLO-22 time quoted in table I is for a final grid of 98 304 cells.

equation in the transformed computational domain becomes so complicated that little is lost in the way of computational efficiency in going to a completely general numerical calculation of the transformation derivatives. The quasi-linear form of the potential equation is conveniently represented under a general coordinate transformation in terms of the contravariant components of the velocity vector. These and the metric tensor of the transformation are calculated numerically at each point. Suitable artificial viscosity terms, modelled after the rotated difference scheme, are added at supersonic points in conservation form, and an iterative scheme is constructed by adding artificial time-dependent terms to simulate a time-dependent process which converges to the steady state solution.

The analysis of FLO-27 is also based on a numerical evaluation of the transformation derivatives at each point, though the sequence of transformations differs from that used in FLO-25. The sequence is the same as that used to transform the equation in the FLO-22 analysis, but preceded by a Joukowsky transformation of the planes normal to the fuselage (cylinder) axis, which reduces the cylinder to a vertical slit. Since the physical coordinates of each mesh point can be calculated from the computational coordinates by simple algebraic operations (i.e., no fractional powers or trigonometric functions need be evaluated), it is efficient to generate the grid as the computation proceeds, rather than store the physical coordinates of each mesh point. The potential equation is differenced in full conservation form, again represented for convenience in terms of the contravariant components of the mass flux density. Suitable artificial viscosity terms are added at supersonic points, and a convergent iteration scheme is constructed to solve the difference equations as in FLO-25.

From a rigorous point of view, only the full conservation form scheme can be justified as correct. Experience with these various approaches in two-dimensional calculations has shown, however, that the quasi-conservative schemes usually produce results very nearly identical to those of the fully conservative codes, and that the nonconservative schemes frequently produce results more nearly consistent with experiment. This latter fact is usually attributed to the tendency for the errors introduced by the nonconservative schemes to be cancelled by the errors introduced by neglect of the shock-wave/boundary-layer interaction. The results of the three approaches seem less different in three-dimensional calculations, and in the absence of a generally-applicable boundary-layer method which properly treats the shock-wave/boundary-layer interaction, it is not clear which approach should be preferred for engineering calculations.

As can be seen from Table I, the computer resources required to run each of these programs are substantial. In addition to basic improvements in the numerical schemes aimed at reducing the cost of running these programs, substantial savings can also be accrued by adapting them to more advanced machines, such as the Control Data STAR-100 at NASA Langley Research Center. The STAR-100 utilizes a pipeline processor which can be programmed to operate very efficiently on large vectors. Improved rates of convergence in the line overrelaxation schemes which are used to solve the difference equations iteratively in these programs are obtained when "new" values of the potential are used as soon as they become available during a sweep of the field. Thus these methods are not as easily

coded for vector processing machines as, say, explicit time-dependent methods. Nevertheless, substantial reductions in run times can be achieved by vectorizing as much of the code as possible. An indication of the improvement achieved by relatively straightforward modification of the relaxation subroutines of FLO-22 to run on the STAR-100 is shown in Table II (ref. 9). The times shown are for 100 relaxation sweeps on each of two grids, with the final grid having 61 × 21 mesh points on each, the upper and lower, wing surface. An improvement in run time by a factor of 3 was achieved over that for the Control Data CYBER 175; further improvement is possible with a more substantial alteration of the code to allow the use of 32-bit words. Also shown is an estimated run time for the Control Data (CDC) 7600, which is about the same as the STAR-100 requirement. Both the STAR-100 and CDC 7600 machines also have the capability of treating even finer grids with their 512 $K_{10}$ Large Core Memory systems (with, of course, an attendant increase in computing time required).

It may also be more efficient to return to iteratively slower numerical methods which lend themselves to more complete vectorization for use on these advanced machines. In a preliminary study using the transonic small-disturbance equation, an explicit method was developed and tested against a conventional successive line overrelaxation (SLOR) scheme. Although the explicit method required more iterations than the SLOR method (by a factor of about 3 on the grids tested), the vector nature of the code allowed reduction of the time required for each iteration on the STAR-100 to one-sixth the time required for each SLOR cycle on the CYBER 175. The net result was a halving of the computing time required for convergence to a specified level of accuracy (ref. 10).

Finally, it should be noted that the results to be presented here, which consist of analyses of given geometric configurations, are only an indication of the number of problems to which these programs have been applied. In particular, FLO-22 has been used by a number of aerospace firms in an iterative cut-and-try mode to design wings as part of test programs still in progress, and which cannot be reported here. In another design application, FLO-22 has been coupled with a geometry-perturbing routine which allows optimization of any aerodynamic parameter (such as shock drag, lift-drag ratio, etc.) under a variety of constraints, either geometric or aerodynamic (ref. 11).

## RESULTS

In this section we shall present results of a number of calculations using these finite-difference programs to predict the aerodynamic characteristics of transport aircraft wings and simple wing-fuselage combinations.

### FLO-22 Results

Results of several calculations using FLO-22 will be shown. The first results to be presented illustrate the effect of the boundary-layer displacement thickness on the (inviscid) pressure distribution, while the last case illustrates a specific application of FLO-22 to predict results for which no data were otherwise available.

Figure 1 presents comparisons at a number of spanwise stations of the calculated streamwise wing-surface pressure distributions with those obtained from experiment (ref. 12) for a low aspect-ratio swept wing panel, with a conventional high-speed section shape, operating in the transonic regime. This wing, designated ONERA M-6, has a leading edge sweep angle of 30°, a taper ratio of 0.7, and a uniform section thickness ratio of 9.8 percent chord, taken streamwise. The experiment was performed with the wing mounted on a wall (i.e, with no fuselage) at a Reynolds number of $18 \times 10^6$, based on the mean aerodynamic chord. The calculation was performed at the same angle of attack and Mach number as the experiment, and no account was taken of viscous effects. As can be seen from the comparison, the agreement is quite good, including the prediction of shock locations and strengths.

Figures 2 and 3 present similar comparisons of calculations and experiment for a supercritical wing tested by the Douglas Aircraft Company in a cooperative program with NASA Ames Research Center (ref. 13). The wing geometry is representative of those being considered for the next generation of subsonic transport aircraft. The wing is twisted both aerodynamically and geometrically, is highly tapered, and has a discontinuity in trailing edge sweep angle at the 35 percent semispan station. The planform has a leading-edge sweep angle of 35 degrees and an aspect ratio of 7. The wing is defined by four distinct streamwise sections (at the 12, 35, 70, and 100 percent semispan stations), whose streamwise thickness ratios vary from 16.3 percent at the root to 11.9 percent at the tip. The experimental data were obtained in the NASA Ames 11-Foot Tunnel at a Reynolds number of $5 \times 10^6$, based on the wing mean aerodynamic chord, with the wing mounted on a fuselage which extended to the 12 percent semispan station of the wing; for the computations the symmetry plane was assumed to be at the same spanwise station as the wing-fuselage junction of the tests. For these calculations, the wing geometry was modified to account for boundary layer effects by adding the displacement thickness obtained from two-dimensional boundary layer calculations multiplied by an empirically determined spanwise weighting factor. The two-dimensional boundary-layer calculations were performed for a typical subcritical pressure distribution for each angle of attack — i.e., no attempt was made to couple the boundary-layer calculation to the details of the supercritical pressure distribution. Nevertheless, agreement between the computed pressure distributions and experimental results is quite good, especially at the lower Mach number, where the assumed boundary-layer model is likely to be more nearly correct.

Figure 4 shows a comparison of calculated and experimental results for a high aspect-ratio supercritical wing tested by NASA Langley. The wing has an aspect ratio of 10.3, is swept 27 degrees at the quarter-chord line, and has streamwise section thickness ratios of 14.9 percent at the fuselage junction, 12 percent at the trailing-edge break, and 10.6 percent at the tip. The experiment was conducted in the Langley 8-foot transonic pressure tunnel at a Reynolds number of $2.4 \times 10^6$, based on the wing mean aerodynamic chord. The model geometry and test conditions are described in References 14 and 15; the data used here are not published in those references, but were taken as part of the test program described there. For this comparison, the interference effect of the fuselage on the wing pressure distribution was approximated by a constant Mach number shift of 0.01; that is, although the experiment was run at

a Mach number of 0.79, the calculation was performed at a Mach number of 0.80. The viscous effect was modelled by a two-dimensional modified Nash-McDonald integral boundary-layer method (ref. 16), taken in streamwise strips. At each span station, boundary-layer transition was assumed to occur at the streamwise location of the transition strips used in the experiment. The viscous and potential calculations were coupled, so that the calculated boundary layer corresponds (within the above-mentioned approximations) to the actual supercritical pressure distribution calculated for the displacement-thickness-modified wing geometry. As can be seen from the figure, the agreement is excellent, except at the inboard stations, where the details of the fuselage interference are almost certainly important. Figure 5 shows the magnitude of the correction to the pressure distribution at the 45 percent semispan station due to the presence of the boundary layer even when the lift has been matched.

The final results to be shown for FLO-22 are those of a calculation used to predict an aerodynamic parameter for which no experimental data (hence, comparisons) were available. A complete calculation coupling the two-dimensional Nash-McDonald strip boundary-layer method with the potential solution was performed to evaluate the relative effectiveness in transonic flow of a 25 percent semispan plain flap (hinged at the 80 percent chord line) on the high aspect ratio, supercritical wing of the previous example (ref. 17). The configuration is shown in Figure 6, along with streamwise wing surface pressure distributions at several spanwise stations. The results are shown for the wing at 1.10 degrees angle of attack in a Mach 0.80 free stream at a Reynolds number of $2.4 \times 10^6$ based on the wing mean aerodynamic chord with the flap undeflected, and with the flap deflected 5 degrees down. The effect of the flap deflection on the spanwise load distribution is shown in Figure 7 for both the initial inviscid calculation and the final solution including the boundary-layer displacement effect. The latter is clearly an important factor which tends to reduce the flap effectiveness by removing some of the effective camber introduced by the flap deflection.

## FLO-25 Results

Calculations with FLO-25 have been carried out thus far only in the inviscid mode; that is, no boundary-layer analysis has been coupled to the program. The results are interesting, however, because, of the three programs in their present forms, this is the only one capable of demonstrating the effects of changes in fuselage cross-sectional area. The configurations tested here consist of a swept wing of moderate aspect ratio, mounted midway on a variety of fuselages. Several of the configurations were tested by NACA in the Ames Research Center 2- by 2-Foot Transonic Wind Tunnel (ref. 18). The wing is untwisted and has a symmetrical NACA $64_2$A015 section in planes perpendicular to the 50 percent chord line. The wing has a taper ratio of 0.5 and the 50 percent chord line is swept back 35 degrees. The fuselages for which calculations were done consist of (1) a Sears-Haack body of fineness ratio 9 having a maximum radius of one-eighth the wing semispan; (2) a modified Sears-Haack body obtained from the first body by removing the exposed wing volume according to the transonic area rule, then scaling the fuselage radii so that the fuselage volume is the same as the original Sears-Haack body; and (3) an infinite cylinder

having a diameter equal to the maximum diameter of the basic Sears-Haack body. The first two bodies were modified to include stings extending to infinity both upstream and downstream. The downstream sting radii were equal to those of the wind-tunnel models tested by NACA; the upstream sting radii were chosen so that the cross-sectional area was a small fraction (five percent) of the fuselage maximum.

Figure 8 demonstrates the effect of the fuselage geometry on the wing pressure distribution. Calculated streamwise pressure distributions at three spanwise stations are compared for the wing on the infinite cylinder and on the basic body at zero degrees angle of attack and a free-stream Mach number of 0.90. The difference is, of course, most pronounced near the fuselage but is still appreciable at the 50 percent semispan station and noticeable near the tip. The effect resembles a Mach number shift, resulting in higher local Mach numbers in the vicinity of the wing for the finite-length fuselage geometry.

Figure 9 illustrates the effect of fuselage area ruling. Streamwise pressure distributions from calculations with the basic and area-ruled fuselages are compared at several span stations, again for a free-stream Mach number of 0.90 and zero degrees angle of attack. The primary overall effect of the area ruling is to reduce the effective Mach number shift caused by the presence of the finite fuselage. The differences in detail which exist from the case of the cylindrical fuselage configuration can only be predicted by a model which takes into account the streamwise variation in fuselage cross section.

Finally, Figure 10 compares the results of the inviscid calculations with experimental measurements for the basic body and the area-ruled configurations (ref. 18). Section pressure distributions were measured at a Reynolds number of $0.96 \times 10^6$ at the 50 percent semispan station, normal to the 50 percent chord line. Results for the same location were interpolated from the nearly streamwise stations at which the solution is calculated. Agreement is quite good, even in the absence of viscous corrections for this relatively simple wing at zero degrees angle of attack, and the effect of the area ruling is clearly predicted.

## FLO-27 Results

The final series of results is for the same high aspect-ratio, supercritical wing as the earlier FLO-22 results, i.e., Figures 4 & 5, but the inviscid flow field is calculated using a fully conservative difference scheme and the fuselage is included as an infinite cylinder of radius equal to the maximum radius of the fuselage on which the wing was mounted in the wind-tunnel tests. The low-mounted position of the test wing was also approximated by mounting the wing low on the cylinder. Calculated results were compared with experiment for two Mach numbers and angles of attack. The angles of attack for which the calculations were performed were determined by matching the spanwise load distributions with those of the experimental data in each case. Comparisons of the calculated and experimentally determined spanwise load distributions for the two cases are shown in Figures 11 and 12. For this calculation, an attempt was made to account for aeroelastic deformation of the model by introducing 0.36 degrees of wash out at the wing tip. This aeroelastic twist

was added linearly from the trailing-edge break to the tip; it was not included in the geometry used in the earlier FLO-22 calculation. As in the FLO-22 calculation, a two-dimensional modified Nash-McDonald integral boundary-layer method was coupled with the inviscid calculation to predict the boundary-layer displacement thickness (ref. 16). Finally, the calculations were performed at slightly higher free-stream Mach numbers than the experiments to attempt to account for the effect of the finite fuselage on which the wind-tunnel model wing was mounted. The value of the Mach number shift of $\Delta M = .007$ was determined by an independent calculation of the transonic potential flow about an axisymmetric body having the same geometric area distribution as the model fuselage (refs. 19,20). Figures 13 and 14 represent charts of the local Mach number at grid points in the computational mesh for two such calculations. In the first, only the fuselage forebody was modelled with the body continuing to downstream infinity as a cylinder with radius equal to the maximum fuselage radius. In the second, the afterbody closure to the sting was also simulated. It is of interest to note that the effective Mach number shift, taken as the weighted average of the local Mach numbers at points in the meridional plane corresponding to the wing projection, is much greater in the latter case. It is also clear from these figures that the representation of the effect of a finite fuselage by a simple Mach number shift is a gross oversimplification: there is not only a large spanwise gradient in the body flow field, but a significant streamwise one as well. A similar Mach number correction, based on a linear subsonic calculation, was used in obtaining the results shown in figures 2 and 3 for the Douglas wing (ref. 13).

As can be seen in Figures 15 and 16 which present the comparisons of streamwise surface pressure distributions at a number of span stations, the agreement near the fuselage is quite good, but there is appreciable error in the predicted shock location at the outboard stations. In the axisymmetric calculation used to estimate the Mach number shift for these calculations, no account was taken of the fuselage boundary layer. Its displacement effect would have been to make the effective Mach number shift larger. This could easily account for the discrepancy in shock position, since the flow field is extremely sensitive to small changes in Mach number at this test condition. Also, oil flow photographs of the model under these test conditions show appreciable spanwise flow in the cove region near the trailing edge of the lower surface, so the discrepancy may be due, in part, to three-dimensional effects in the boundary layer which are neglected.

## CONCLUSIONS

In this final section, we shall attempt to draw some general conclusions which will point naturally to areas in which additional work should be continued. In general, the success of FLO-22 in predicting pressure distributions that agree well with experiment when fuselage interference effects are not important provides strong motivation for continued development of the geometrically more general finite-volume codes. The numerical evaluation of the metric results in a loss of accuracy relative to the analytical transformation method. This penalty appears inescapable for the treatment of general configurations, and the results of the pilot codes indicate that the loss of accuracy is not too severe as long as a reasonably fine grid is used.

It has been clear for some time that an accurate simulation of the boundary layer is important for the sensitive supercritical airfoil geometries. They have substantial aft camber, the effect of which can be drastically altered by boundary-layer growth, which produces significant changes in the predicted inviscid lift. Two-dimensional strip boundary-layer methods appear to do well in many cases near cruise design conditions. However, there are also cases where significant spanwise flows might be important. To assess the importance of these effects (e.g., the spanwise flow in the lower surface cove of the NASA high aspect-ratio, supercritical wing), a fully three-dimensional boundary-layer code should be coupled to the transonic potential flow calculation. Such an effort is currently underway, using FLO-27 for the inviscid calculation, in a program sponsored by the NASA Langley Research Center.

Planned future developments of the inviscid codes can be grouped into two general classes. The first deals with extensions of the geometric capabilities of the codes. A program is currently underway to allow calculation of the flow past a wing mounted on a finite length fuselage, as well as improved output capabilities of the programs. In the longer range, the grid generation schemes must be generalized to allow treatment of the tail effects and the engine pylon/nacelle effects. The second general class of problems deals with improvements in the basic numerical methods themselves, with the goal of reducing the computer resources required to provide answers with adequate accuracy. Methods for accelerating the convergence of the iterative schemes (to reduce the computing time required) and for incorporating shock fitting techniques (to reduce the amount of storage required as well) are currently under study, as well as continued efforts to best adapt these codes to the next generation of vector-processing computers.

Langley Research Center
National Aeronautics and Space Administration
Hampton, VA 23665
June 8, 1978

## REFERENCES


1. Garabedian, P. R.; and Korn, D. G.: Analysis of Transonic Airfoils. Commun. Pure & Appl. Math., vol. 24, no. 6, Nov. 1971, pp. 841-851.

2. Jameson, Antony: Transonic Flow Calculations for Airfoils and Bodies of Revolution. Rep. 390-71-1, Grumman Aerospace Corp., 1971.

3. Caughey, D. A.; and Jameson, Antony: Accelerated Iterative Calculation of Transonic Nacelle Flowfields. AIAA J., vol. 15, no. 10, Oct. 1977, pp. 1474-1480.

4. Jameson, Antony: Iterative Solution of Transonic Flows Over Airfoils and Wings, Including Flows at Mach 1. Commun. Pure & Appl. Math., vol. XXVII, no. 3, May 1974, pp. 283-309.

5. Jameson, Antony; and Caughey, D. A.: Numerical Calculation of the Transonic Flow Past a Swept Wing. COO-3077-140, ERDA Math. & Comput. Lab., New York Univ., June 1977. (Also available as NASA CR-153297.)

6. Caughey, D. A.; and Jameson, Antony: Numerical Calculation of Transonic Potential Flow About Wing-Fuselage Combinations. AIAA Paper 77-677, June 1977.

7. Jameson, Antony; and Caughey, D. A.: A Finite Volume Method for Transonic Potential Flow Calculations. AIAA 3rd Computational Fluid Dynamics Conference, June 1977, pp. 35-54.

8. Caughey, D. A.; and Jameson, Antony: Calculation of Transonic Potential Flowfields About Complex, Three-Dimensional Configurations. Proceedings of the Workshop on Transonic Flow Problems in Turbomachinery, Hemisphere Pub. Corp., 1977, pp. 274-293.

9. Smith, Robert E.; Pitts, Joan, I.; and Lambiotte, Jules J.: A Vectorization of the Jameson-Caughey NYU Transonic Swept-Wing Computer Program FLO-22-VI for the STAR-100 Computer, NASA TM-78665, 1978.

10. Keller, James D.; and Jameson, Antony: Preliminary Study of the Use of the STAR-100 Computer for Transonic Flow Calculations. NASA TM-74086, 1977.

11. Hicks, Raymond M.; and Henne, Preston A.: Wing Design by Numerical Optimization. [Paper] 77-1247, American Inst. Aeronaut. & Astronaut., Aug. 1977.

12. Monnérie, B.; and Charpin, F.: Essais de Buffeting d'une Aile en Flèche en Transonique. 10$^{e}$ Colloque d'Aerodynamique Appliquée, Institute de Mechanique des Fluides, Lille, Nov. 1973. (Available in English translation as NASA TT F-15803.)

13. Henne, P. A.; and Hicks, R. M.: Wing Analysis Using a Transonic Potential Flow Computational Method. NASA TM-78464, 1978.

14. Bartlett, Dennis W.: Wind-Tunnel Investigation of Several High Aspect-Ratio Supercritical Wing Configurations on a Wide-Body-Type Fuselage. NASA TM X-71996, 1977.

15. Bartlett, Dennis W.; and Patterson, James C., Jr.: NASA Supercritical-Wing Technology. NASA TM-78731, 1978.

16. Newman, Perry A.; Carter, James E.; and Davis, Ruby M.: Interaction of a Two-Dimensional Strip Boundary Layer With a Three-Dimensional Transonic Swept Wing Code. NASA TM-78640, 1978.

17. Perry, Boyd, III: Control-Surface Hinge-Moment Calculations for a High-Aspect-Ratio Supercritical Wing. NASA TM-78664, 1978.

18. McDevitt, John B.: An Experimental Investigation of Two Methods for Reducing Transonic Drag of Swept-Wing and Body Combinations. NACA RM A55B21, 1955.

19. South, Jerry C., Jr.; and Jameson, Antony: Relaxation Solutions for Inviscid Axisymmetric Transonic Flow Over Blunt or Pointed Bodies. AIAA Computational Fluid Dynamics Conference, July 1973, pp. 8-17.

20. Keller, James D.; and South, Jerry C., Jr.: RAXBOD: A Fortran Program for Inviscid Transonic Flow Over Axisymmetric Bodies. NASA TM X-72831, 1976.

TABLE I. FEATURES OF 3-D TRANSONIC POTENTIAL FLOW PROGRAMS.

| NAME | CAPABILITY | REMARKS | CPU MIN CYBER 175 | STORAGE | STATUS |
|---|---|---|---|---|---|
| FLO-22 | ISOLATED SWEPT OR YAWED WINGS | NONCONSERVATIVE, SHEARED PARABOLIC COORDINATES | 26 (61 x 21 ON WING) | $80K_{10}$ CORE PLUS EXTERNAL DISK | PRODUCT-ION CODE |
| FLO-25 | SWEPT WING ON FUSELAGE OF SLOWLY-VARYING CIRCULAR CROSS-SECTION | QUASI-CONSERVATIVE FINITE VOLUME | 40 ESTIMATED (51 x 21 ON WING) | $100K_{10}$ CORE PLUS EXTERNAL DISK | PILOT CODE |
| FLO-27 | SWEPT OR YAWED WINGS AND WING-CYLINDER | CONSERVATIVE FINITE VOLUME | 33 (51 x 21 ON WING) | $90K_{10}$ CORE PLUS EXTERNAL DISK | PILOT CODE |

TABLE II. COMPUTING TIMES FOR FLO-22 ON ADVANCED COMPUTERS (192 x 16 x 32 MESH)

| COMPUTER | CPU MIN | REMARKS |
|---|---|---|
| CYBER 175 | 26 | FINER MESH IMPOSSIBLE WITH SMALL $131K_{10}$ CORE |
| CDC 7600 | 9 | CAN DO 295 x 18 x 35 WITH $512K_{10}$ LCM |
| STAR-100 | 10* | CAN DO 300 x 32 x 32 WITH $512K_{10}$ CORE |

* FURTHER REDUCTION POSSIBLE USING 32-BIT WORDS

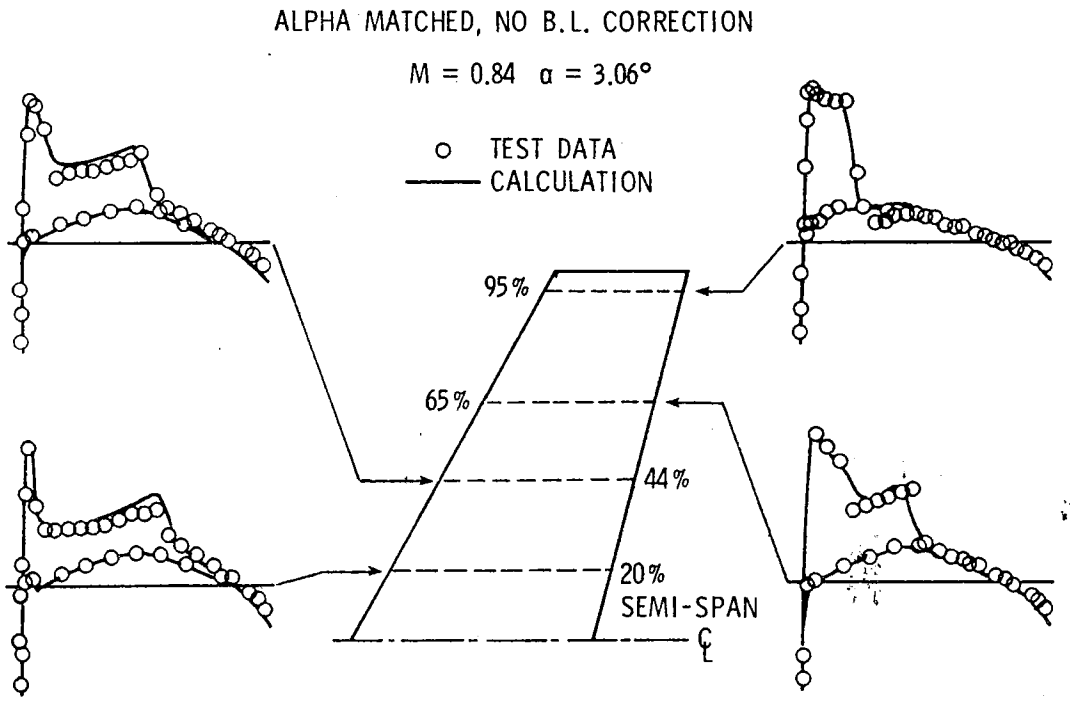


Figure 1.- Comparison of FLO-22 results with experiment for ONERA wing M-6; test conducted at $R_c = 18 \times 10^6$.

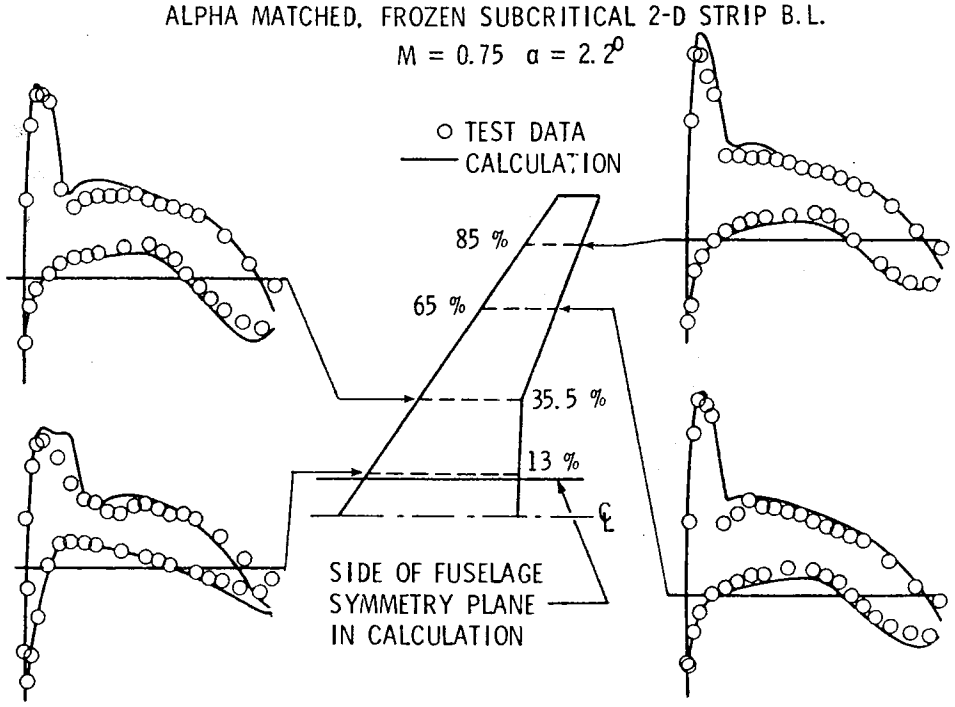


Figure 2.- Comparison of FLO-22 results with experiment for Douglas supercritical wing; test conducted at $R_c = 5 \times 10^6$.

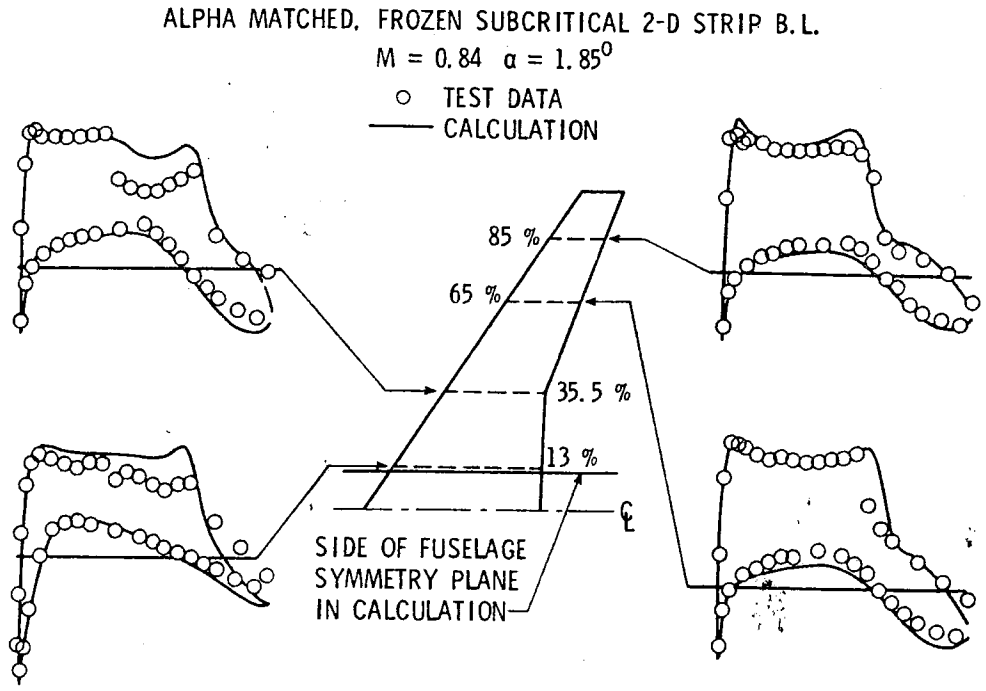


Figure 3.- Comparison of FLO-22 results with experiment for Douglas supercritical wing; test conducted at $R_{\bar{c}} = 5 \times 10^6$.

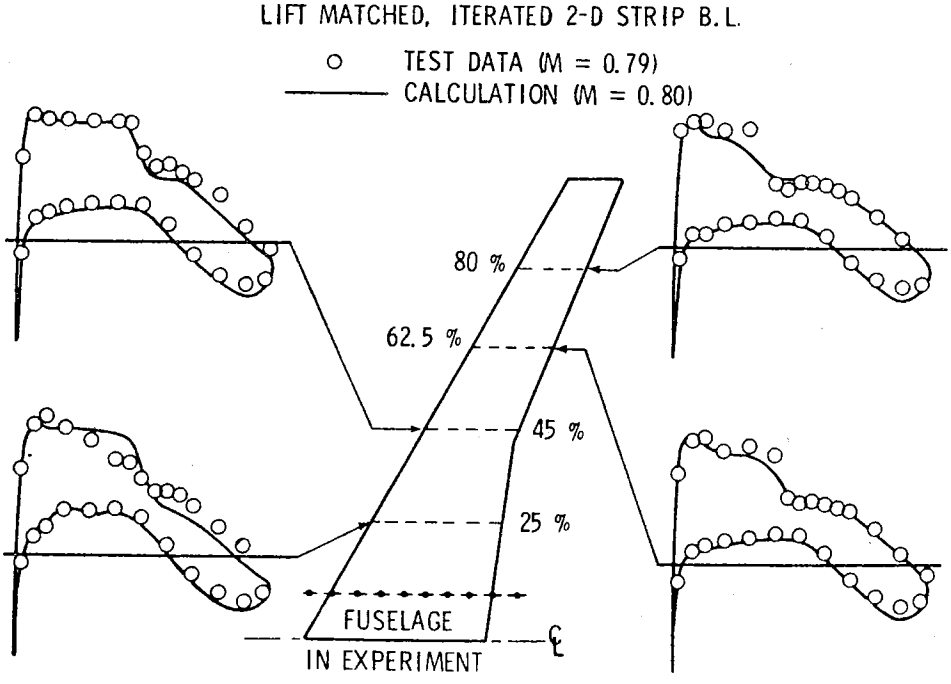


Figure 4.- Comparison of FLO-22 results with experiment for NASA supercritical wing; test conducted at $R_{\bar{c}} = 2.4 \times 10^6$.

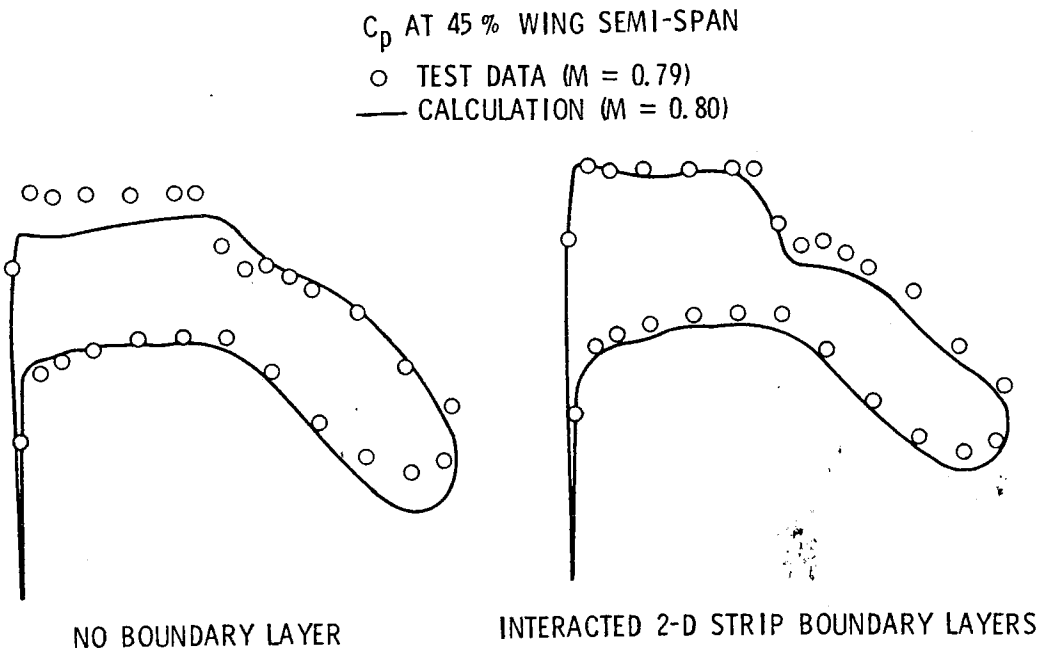


Figure 5.- Effect of boundary-layer displacement thickness on inviscid pressure distribution for NASA supercritical wing with lift matched; FLO-22 calculations and test at $R_c = 2.4 \times 10^6$.

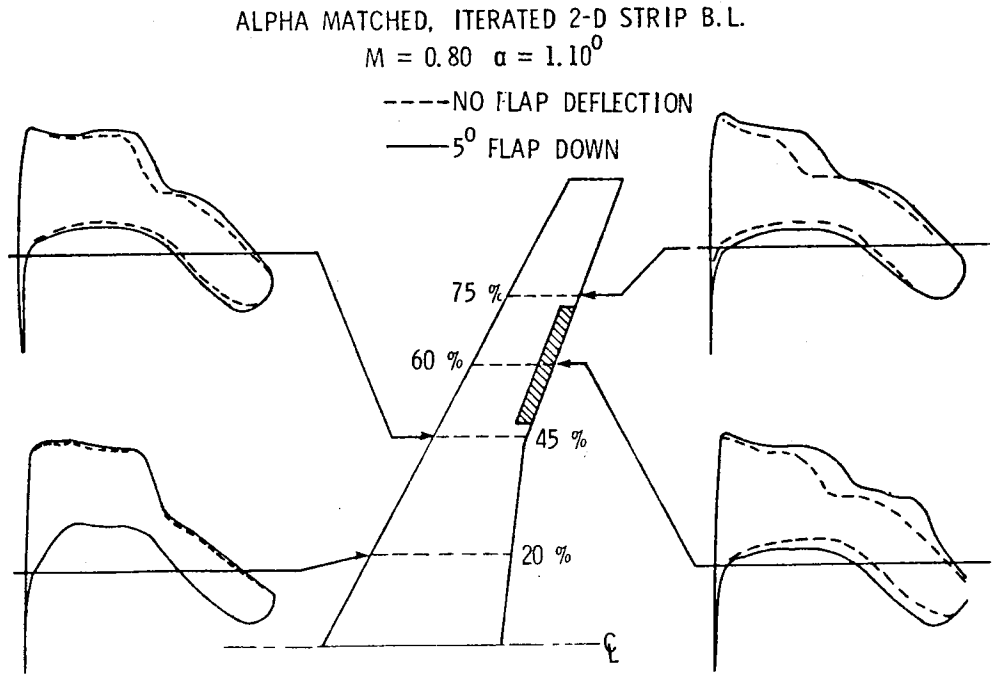


Figure 6.- Effect of flap deflection on FLO-22 calculated pressure distribution for NASA supercritical wing at $R_c = 2.4 \times 10^6$.

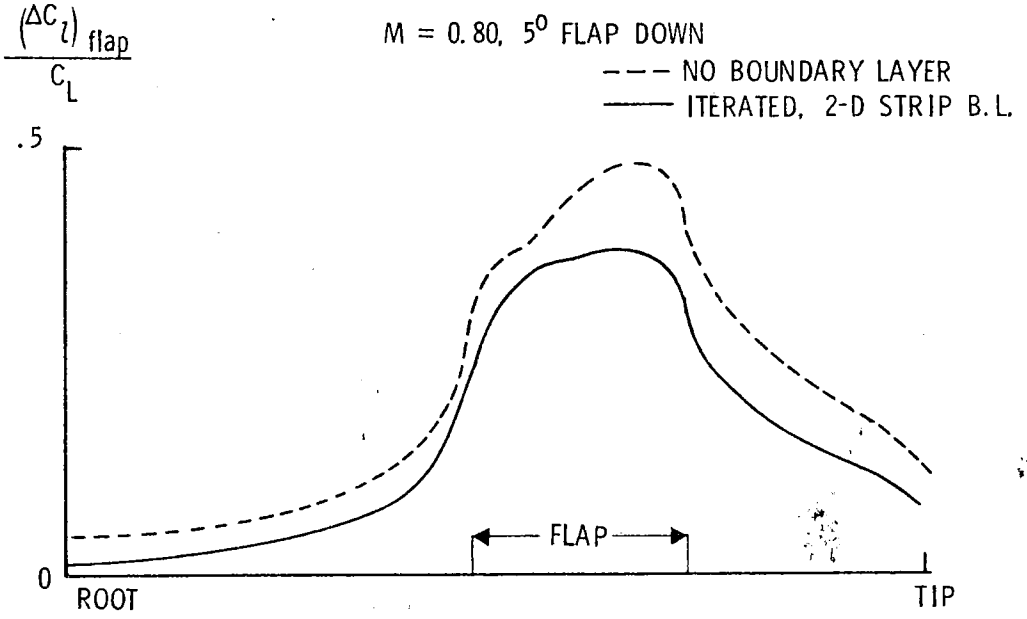


Figure 7.- FLO-22 calculated spanwise distribution of lift increment due to flap deflection on NASA supercritical wing, showing influence of boundary layer at $R_c = 2.4 \times 10^6$.

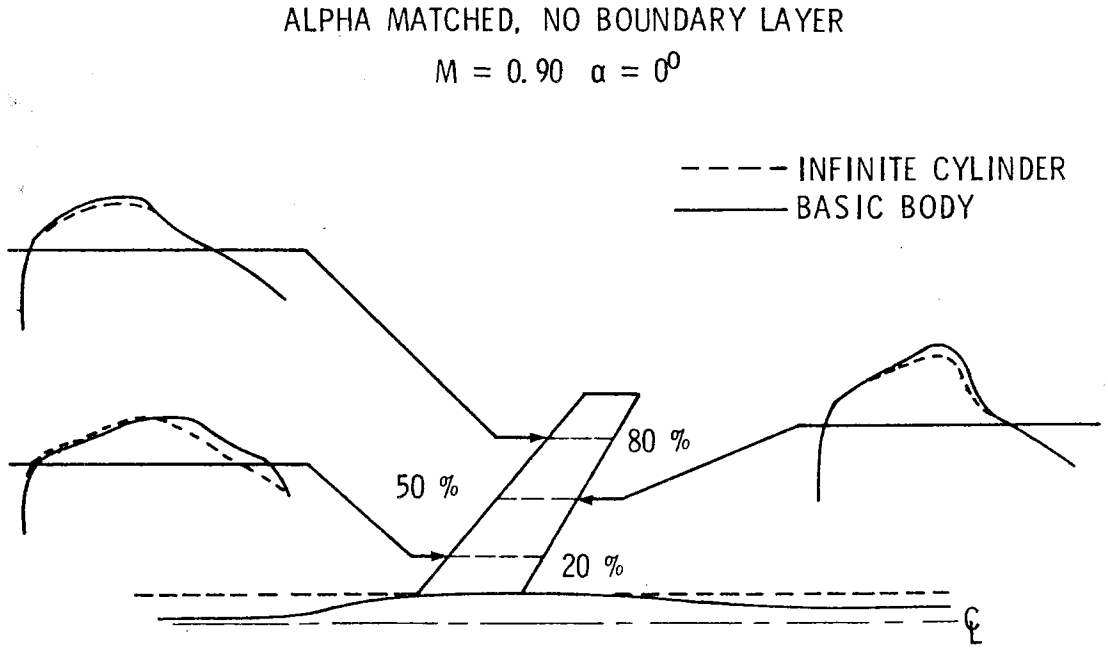


Figure 8.- Comparison of FLO-25 results for wing mounted on cylindrical and Sears-Haack bodies, showing influence of finite-length body.

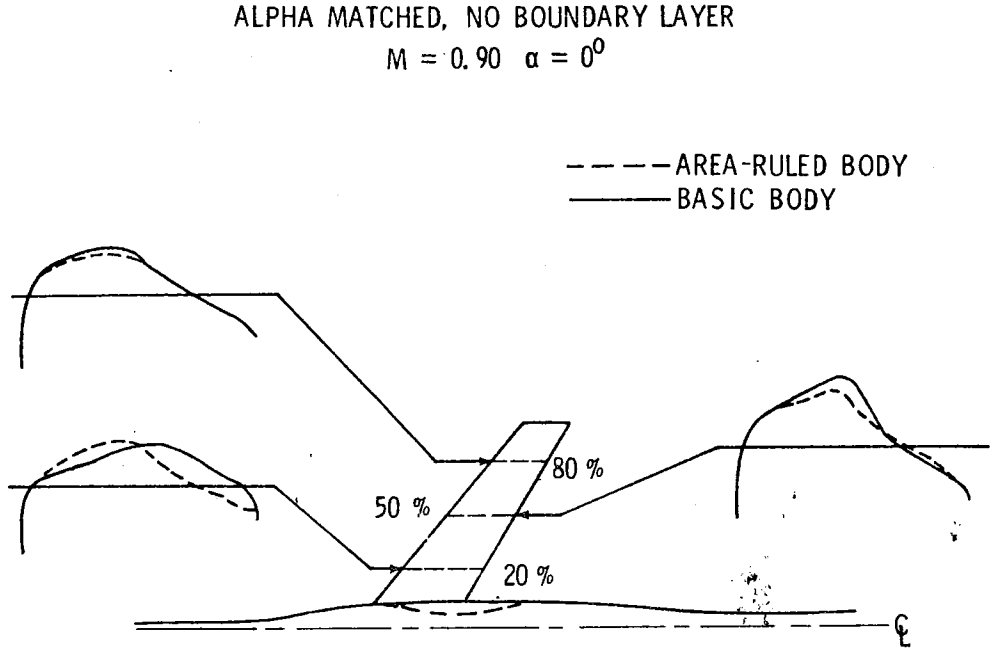


Figure 9.- Comparison of FLO-25 results for wing mounted on Sears-Haack and area-ruled bodies, showing influence of area-ruled body.

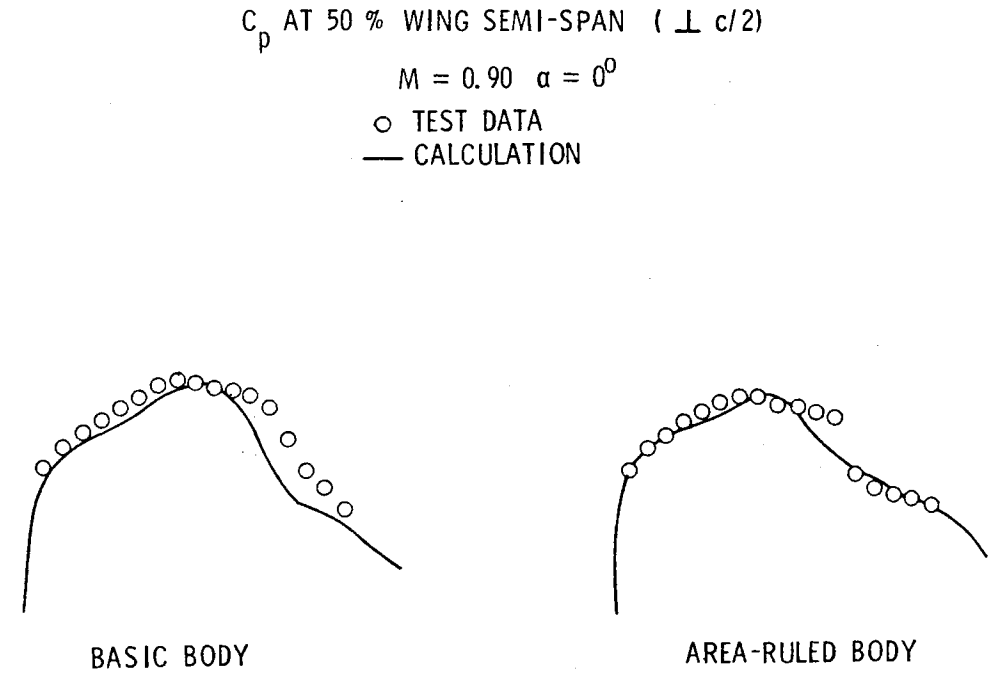


Figure 10.- Comparison of FLO-25 results with experiment for wing mounted on Sears-Haack and area-ruled bodies; test conducted at $R_c = 0.96 \times 10^6$.

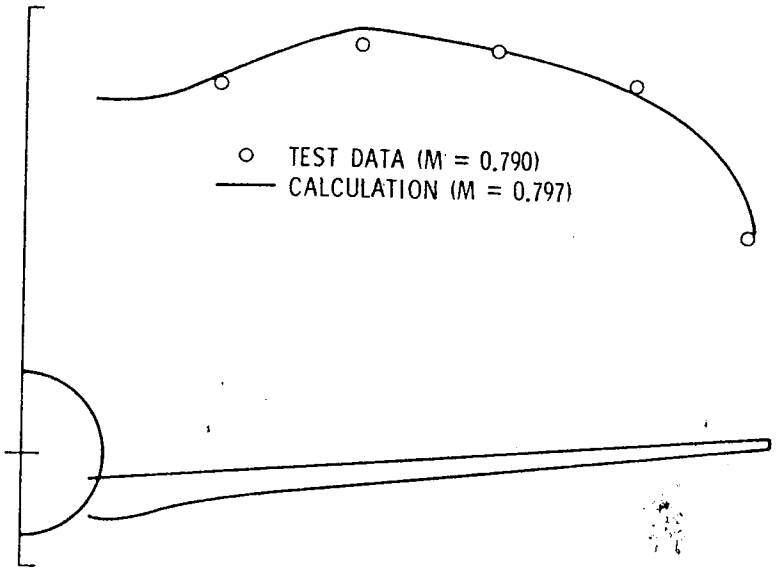


Figure 11.- Comparison of spanwise normal force distributions on NASA supercritical wing with lift matched; FLO-27 calculations and test at $R_c = 2.4 \times 10^6$.

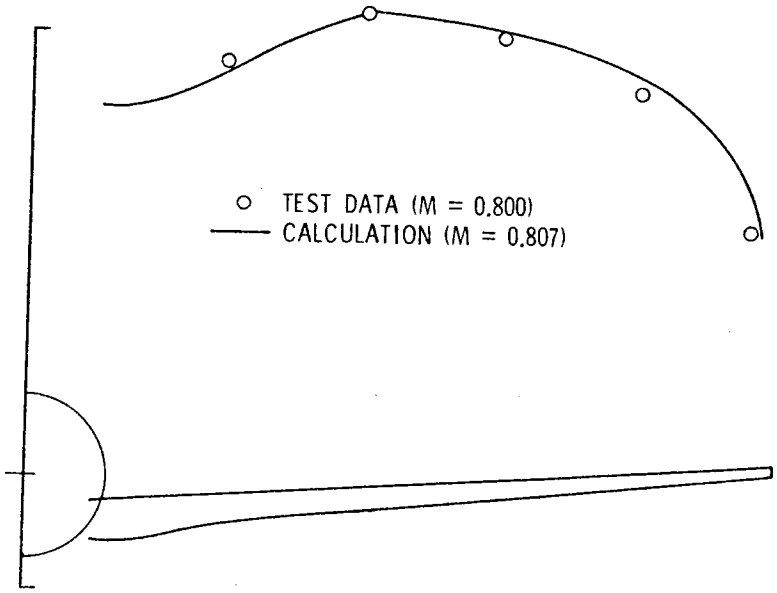


Figure 12.- Comparison of spanwise normal force distributions on NASA supercritical wing with lift matched; FLO-27 calculations and test at $R_c = 2.4 \times 10^6$.

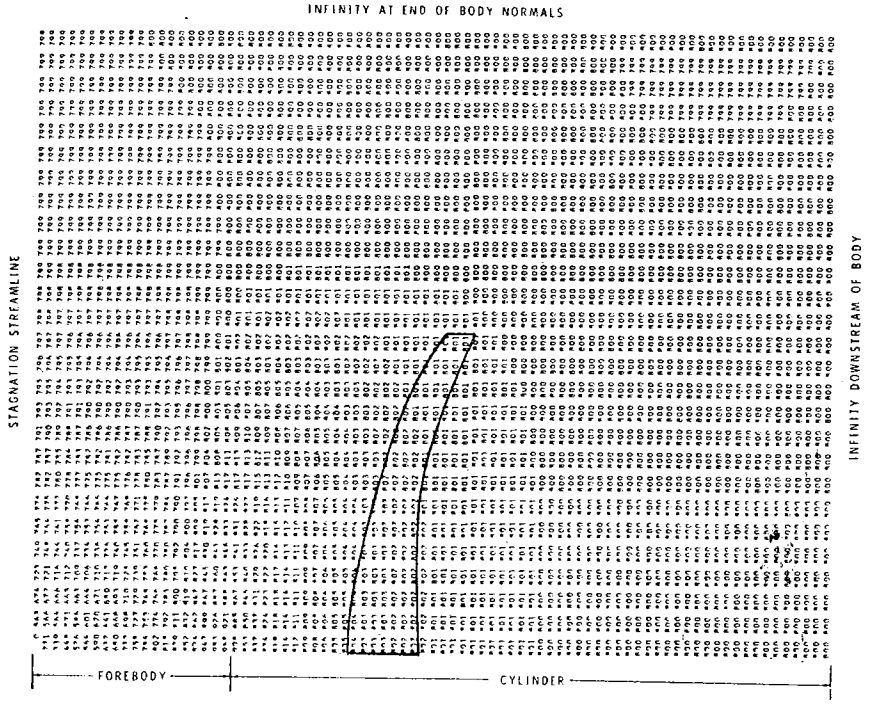


Figure 13.- Chart of local Mach numbers at mesh points in computational plane for axisymmetric flow about forebody-cylinder combination. Wing planform indicated by solid line.

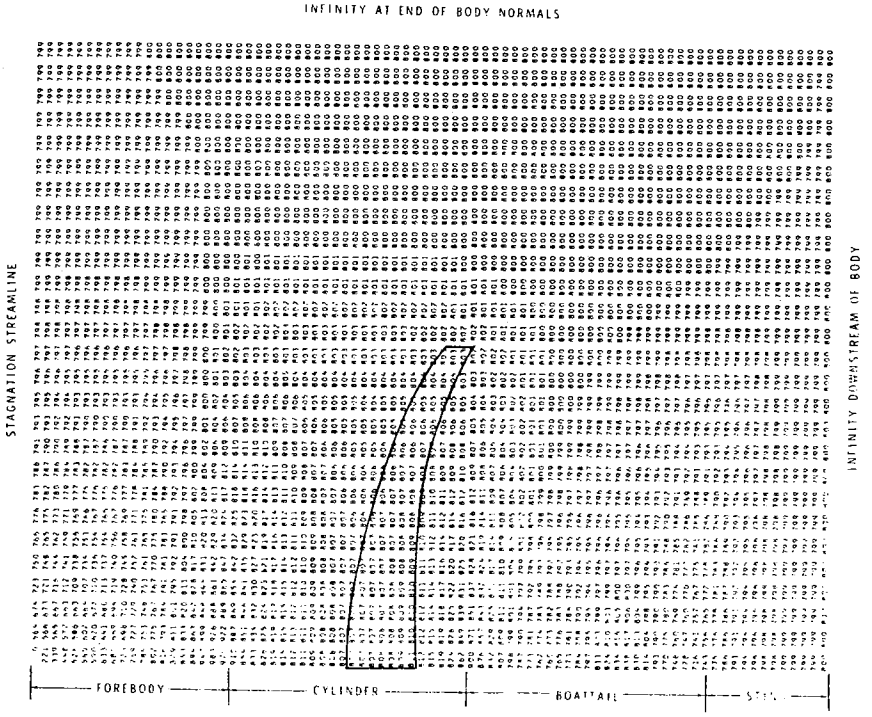


Figure 14.- Chart of local Mach numbers at mesh points in computational plane for axisymmetric flow about forebody-cylinder-boattail-sting combination. Wing planform indicated by solid line.

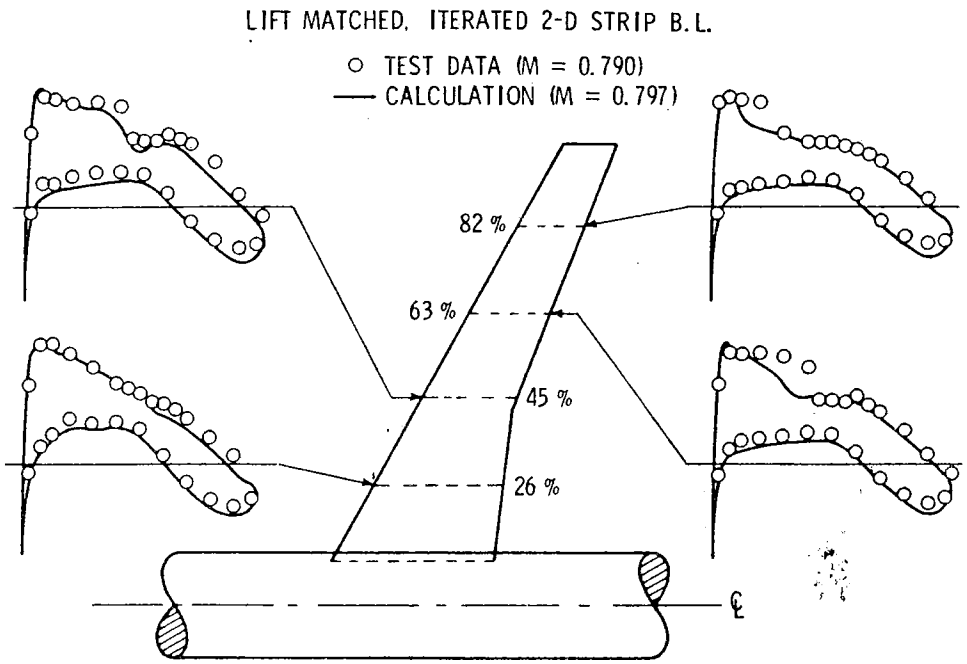


Figure 15.- Comparison of FLO-27 results with experiment for NASA supercritical wing; test conducted at $R_c = 2.4 \times 10^6$.

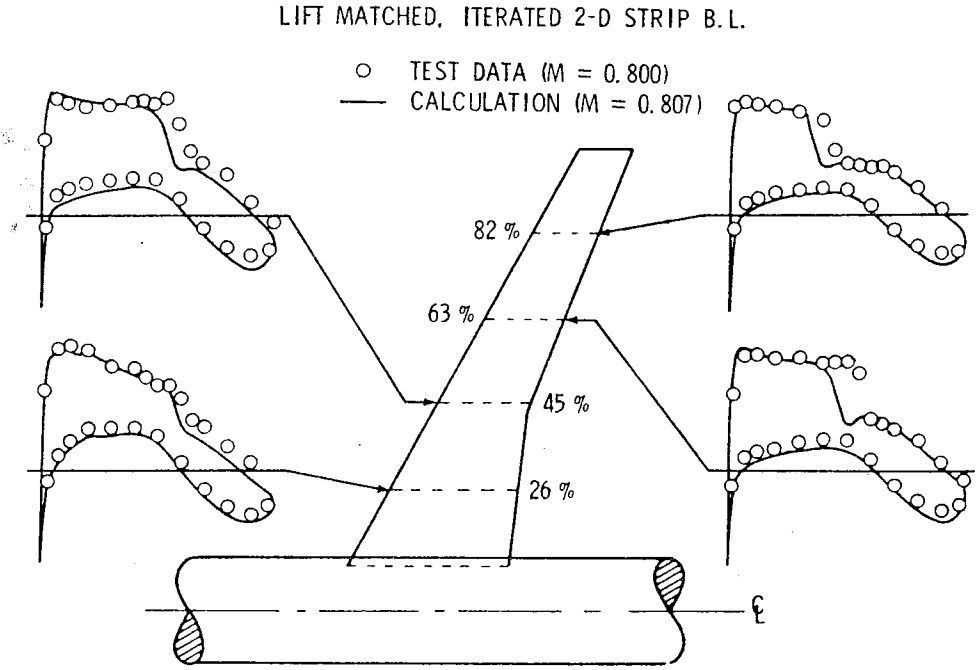


Figure 16.- Comparison of FLO-27 results with experiment for NASA supercritical wing; test conducted at $R_c = 2.4 \times 10^6$.

| 1. Report No. | 2. Government Accession No. | 3. Recipient's Catalog No. |
|---|---|---|
| NASA TM-78733 | | |

| 4. Title and Subtitle | 5. Report Date |
|---|---|
| RECENT EXPERIENCES WITH THREE-DIMENSIONAL TRANSONIC POTENTIAL FLOW CALCULATIONS | July 1978 |
| | 6. Performing Organization Code |
| 7. Author(s) | 8. Performing Organization Report No. |
| David A. Caughey, Perry A. Newman, and Antony Jameson | L-12359 |
| | 10. Work Unit No. |
| 9. Performing Organization Name and Address | 505-06-13-01 |
| NASA Langley Research Center<br>Hampton, VA 23665 | 11. Contract or Grant No. |
| | 13. Type of Report and Period Covered |
| 12. Sponsoring Agency Name and Address | Technical Memorandum |
| National Aeronautics and Space Administration<br>Washington, DC 20546 | 14. Sponsoring Agency Code |

15. Supplementary Notes

This paper was presented at the CTOL Transport Technology Conference held at Langley Research Center on February 28 to March 3, 1978.
David A. Caughey: Assistant Professor, Cornell University.
Antony Jameson: Professor, New York University.
This work was sponsored in part by NASA under Grants NGR 33-016-167 and NGR 33-016-201 and by the Office of Naval Research under Contracts N00014-77-C-0033 and N00014-77-C-0032.

16. Abstract

Some recent experiences with computer programs capable of solving finite-difference approximations to the full potential equation for the transonic flow past three-dimensional swept wings and simple wing-fuselage combinations are discussed. The programs which have been used are (1) a nonconservative program for swept wings (FLO-22), (2) a quasi-conservative finite-volume program capable of treating swept wings mounted on fuselages of slowly varying circular cross section (FLO-25), and (3) a fully conservative finite volume scheme capable of treating swept wings and wing-cylinder combinations (FLO-27). The present capabilities of these codes are reviewed. The relative merits of the conservative and nonconservative formulations are discussed, and the results of calculations including corrections for the boundary-layer displacement effect are presented. The potential impact of the programs on design will be assessed, considering questions of accuracy, computer cost, and geometric capability, both for the current codes and planned future developments.

| 17. Key Words (Suggested by Author(s)) | 18. Distribution Statement |
|---|---|
| Aerodynamics<br>Transonic flow<br>Supercritical wings | FEDD Distribution<br><br>Subject Category 02 |

| 19. Security Classif. (of this report) | 20. Security Classif. (of this page) | 21. No. of Pages | 22. Price* |
|---|---|---|---|
| Unclassified | Unclassified | 21 | $4.00 |

Available: NASA's Industrial Application Centers

NASA-Langley, 1978